



IJRASET

International Journal For Research in
Applied Science and Engineering Technology



INTERNATIONAL JOURNAL FOR RESEARCH

IN APPLIED SCIENCE & ENGINEERING TECHNOLOGY

Volume: 6 Issue: IV Month of publication: April 2018

DOI: <http://doi.org/10.22214/ijraset.2018.4618>

www.ijraset.com

Call:  08813907089

E-mail ID: ijraset@gmail.com

Effect of Mn^{2+} ions on Structural and Magnetic properties of Co-precipitated Ni-Cr nano ferrite for Potential applications as MRI Contrast agent

S. Sukandhiya¹, B. Uthayakumar², S.Periandy³, J. Suryakumary⁴, R. Roja⁵

^{1, 2, 4, 5}(Research Scholar, Department of Physics, Kanchi Mamunivar center for PG Studies, Puducherry, India)

³(Associate Professor, Department of Physics, Kanchi Mamunivar center for PG Studies, Puducherry, India)

Abstract: Manganese doped Nickel-Chromium nano ferrites has been prepared by Co-precipitation method with pH as 10. Effect of doping Manganese ($x = 0.0, 0.2, 0.4, 0.6, 0.8$ and 1.0) on structural and magnetic properties are reported in the present work. All samples are sintered at 1173 K and characterized. X-ray Diffraction (XRD) used to reveal phase and structural parameters. Morphology has been obtained from Scanning Electron Microscope. Compositions of the synthesized samples are scaled with Energy Dispersive X-ray Spectroscopy (EDX/EDS). FTIR is equipped to record vibration of nanoferrite sites and two prominent absorption bands ν_1 and ν_2 corresponding to the stretching vibration of tetrahedral and octahedral sites around $614-582\text{ cm}^{-1}$ and $420-443\text{ cm}^{-1}$. The magnetic parameter such as Saturation magnetization (M_s), Remanent magnetization (M_r), Coercive field (H_c) and Squareness ratio are determined by Vibrational Sample Magnetometer (VSM). The average crystallite size calculated from XRD pattern and it ranging between 44 and 55 nanometers. Lattice constant of the samples lies in between 8.4407 \AA and 8.6615 \AA . The magnetic parameters changes non-linearly with respect to increase in concentration of Manganese ions. Maximum Anisotropy constant obtained at $x = 0.6$ is $11488.49\text{ (erg/cm}^3\text{)}$. Bohr magneton value is maximum for 0.4 concentration with 3.036.

Keywords: Mn doped Ni-Cr nano ferrite, Co-Precipitation method, Magnetic Properties

I. INTRODUCTION

Ferrites are extensively used for technological application due to their potential electrical and magnetic properties. In the midst of the various types of ferrites particularly spinel ferrite with general formula MFe_2O_4 disseminates more interest among the researcher for the past few decades, due to their immense properties. Spinel structure belongs to $Fd3m$ space group having cubical close packing of 32 oxygen anions along with 24 cations. The 8 cations are located in tetrahedral sites and rest at 16 octahedral sites. Normal spinel and inverse spinel are two forms of spinel structure. In normal spinel structure, all divalent ions occupy tetrahedral sites, while in inverse spinel structure divalent ions have preference for octahedral sites. Structural formula for spinel ferrites is: $[M_{1-i}Fe_i]^A [M_iFe_{2-i}]^B O_4$, where i is the inversion parameter (0 for normal and 1 for inverse spinel). If divalent ions get distributed between tetrahedral and octahedral sites, the spinel ferrite becomes partially inverted [1-3]. In particular Nano ferrites are novel in comparison with the corresponding bulk part such as superparamagnetism, high surface area, large surface-to-volume ration and easy separation under external magnetic field and strong adsorption ability. They have promising applications in electrical components, memory devices, magnetostriction, microwave devices and high-density magnetic recording [4].

Generally magnetic nano particles have the potential to produce heat under an alternating magnetic field, this special property fascinated the researcher to do work on this field. During magnetization reversal, energy loss occurs this phenomenon paved the base for promising application of magnetic nano particles in biomedicine known as Magnetic Fluid Hyperthermia MFH and Targeted Drug Delivery system. Hyperthermia is a minimally invasive method for cancer therapy in which the target tissues are annealed to about $42-46^\circ\text{C}$. Heat treatment in such temperature range is cytotoxic for tumor cells because of their unsystematic and compact vascular structure that promotes an unfavorable microenvironment inside them. Thus tumors are already stressed by low oxygen, inadequate blood supply, higher than normal acid concentration and insufficient nutrients. These cancer cells are less able to tolerate the added stress of heat than a healthy cell in normal tissues [5-9]. A strategy to achieve constant hyperthermic efficiency, by synthesizing novel combination of ferrite with increased magnetic anisotropy.

Zhao et al, [10] studied the effect of Fe^{3+} ions substitution by rare earth ions and effect of calcination on magnetic properties of Mn-Ni nano ferrite by emulsion method and reported that addition of rare earth ion and calcination affects the structural and magnetic behaviour of the parental composition. E.R.Kumar et al substituted Mn ions in Nickel ferrite through auto combustion method and

investigated the structural, magnetic and dielectric properties corresponding to the concentration of Mn ion in the sample and corresponding to the fuel variation used in the synthesis process [11]. R.D.Misra et al compared Saturation Magnetization values of Nickel, Zinc and Manganese ferrite and reported M_s as 25 emu/g, 8 emu/g, 6 emu/g respectively [12]. Mn-Ni nano ferrite which is regarded as mixed ferrite of the both Manganese and Nickel ferrite. Manganese ferrite has partially inverse spinel structure in which 80% of Mn^{2+} has strong tendency to occupy tetrahedral (A) sites while the remaining 20% occupies octahedral (B) sites in the form of Mn^{3+} [13] and Fe^{3+} ions are distributed between A and B sites. Ni^{2+} ions occupy octahedral (B) sites. Presence of Anti-ferromagnetic Cr^{3+} ions with strong B site preference could produce sufficient changes in the structure of Manganese-Nickel ferrite. Wide-range of literature survey has been done and a novel composition of Mn-Ni-Cr nanoferrite ($x = 0$ to 1.0 in steps of 0.2) synthesized by Co-precipitation method is not reported yet and in this paper we devoted to the influence of concentration of Manganese on structural and magnetic properties of Manganese doped Nickel-Chromium ferrite by Co-precipitation method. Current study is to reveal the physio-chemical behavior on addition of Mn^{2+} ion.

II. MATERIALS AND METHODS

A. Material for production

Magnetically potential Manganese doped Nickel-Chromium nano ferrites at various concentration of Mn ion has been prepared from the starting materials $MnCl_2 \cdot 4H_2O$, $NiCl_2$, $CrCl_3 \cdot 6H_2O$, $FeCl_3 \cdot 6H_2O$ and NaOH. Analytical grade of these precursors are purchased from SIGMA ALDRICH, Germany with 98% purity.

B. Synthesis Methodology

A fruitful synthesizing methodology involves correct choice of precursor, its composition and reaction environment. Particularly for wet chemical methods like sol-gel, hydrothermal, co-precipitation and colloid emulsion technique, pH controller plays an important role. For the present work eco friendly NaOH is used to maintain pH. The physio-chemical properties of nanoparticles are greatly influenced by particle size, morphology, purity and chemical composition. Chemical method has been conformed to efficiently control the morphology and chemical composition of prepared nano powder. Among wet chemical techniques sol-gel, hydro thermal and colloid emulsions are time consuming and involve highly unstable alkoxides and difficult to maintain reaction conditions. Co-precipitation is one of the more successful techniques for synthesizing ultrafine nanoparticles having narrow particle size distribution [14]. These advantages on Co-precipitation method motivated authors to synthesize $Mn_xNi_{1-x}Cr_{0.5}Fe_{1.5}O_4$ ($x = 0, 0.2, 0.4, 0.6, 0.8, 1.0$) nano ferrites by Co-precipitation method. The precursors for Fe ion are taken as 2 M and 1M for other Metals chlorides. They are mixed in stoichiometric ratio and added one by one on the basis of their electronegativity value. Mixture of Aqueous solution is stirred rigorously at 338K for 30 minutes, meanwhile NaOH is added to the brain solution by drop by drop using a burette till solution reaches pH value 10. The required composition of nano ferrites are formed from conversion of metal salt into hydroxide and then transformed into ferrites. The precipitates obtained were thoroughly washed more than three times with double distilled water and acetone. The final product were dried and sintered at 1173 K for the formation of spinel ferrite crystal structure.

C. Physical measurements

Crystal structure of all the samples were examined by powder X-Ray diffraction XRD patterns at room temperature PANalytical-X'Pert PRO powder diffractometer using $Cu-K\alpha_1$ radiation. Scanning Electron Microscopy (SEM) study was performed by VEGA 3 TESCAN Scanning Electron Microscope, operated at 120 KV. Elemental analysis has been done with BRUKER EDS. Fourier Transform Infrared (FT-IR) spectra were recorded on SHIMADZU FT-IR spectrophotometer using KBr pellet method in the range $4000-400\text{ cm}^{-1}$. The magnetic properties were measured at room temperature by LAKESHORE vibrating sample magnetometer (VSM).

III. RESULT AND DISCUSSION

A. X - Ray Diffraction analysis

Fig.1 shows x-ray diffraction pattern of Manganese doped Nickel-Chromium nano ferrite for the concentration $x = 0, 0.2, 0.4, 0.6, 0.8$ and 1.0. Major peaks (220), (311), (400), (422), (511) and (440) are present in XRD pattern of all the samples which reveals these are having the disordered spinel ferrite formation of space group $Fd\bar{3}m$, with Fe^{3+} in tetrahedral (8c) and octahedral (12d) sites whereas Ni^{2+} and Mn^{2+} ions occupy the octahedral position [15]. These matches with the JCPDS file No.10-0325, No.85-2456 and No.75-00894. Minor secondary phase reflections (331) and (310) peaks corresponding to Cr_2O_3 and $\alpha-Fe_2O_3$ are observed for the samples except 0 and 1 concentration. This secondary phase of Cr_2O_3 and alpha Fe_2O_3 is due to John-teller distortion caused by the

John teller ions Ni^{2+} and Mn^{2+} which will be the major reason for secondary phase formation. Increase in Mn^{2+} ion cause more john teller distortion in the nanoferrite due degeneracy of electronic level of this ion. In addition to major peaks, minor reflections peaks from the planes (111), (222), (422), and (620) are present in all samples except $x = 0.4$ (222) is absent and for 0.6 (620) is absent. Disappearance of minor reflection peaks is due to slight amorphization of sample [16,17].

Generally intensity of XRD peaks corresponds to the crystalline nature of the samples. For undoped Ni-Cr nano ferrite, intensity of XRD peaks higher than all other samples. Addition of higher ionic radius Mn^{2+} ion ($r_{\text{Mn}} = 0.89 \text{ \AA}$) in Ni-Cr nano ferrite which will increase the lattice constant and results in peak shift towards lower reflection angle. Increase in Manganese concentration decreases the crystalline nature, which results in decrease in XRD peak intensity. Intensity and peak width of XRD pattern related to particle size and crystallinity of the samples. The intensities of (220) and (440) planes are more sensitive to cations in tetrahedral and octahedral sites respectively [18,19]. From TABLE 1 it is clear that intensity of (440) and (220) varies nonlinearly with increase in Mn^{2+} ion, this is due to presence of Fe^{2+} ion in octahedral site formed due to reduction of Fe^{3+} ion to Fe^{2+} for higher Manganese concentration causes migration of ions and also decrease in Nickel at octahedral site [20].

Average crystallite size 'D' and lattice constant has been estimated from X-ray reflections indexed (111), (220), (311), (222), (400), (422), (511), (440) and (620), using Scherer's equation $D = 0.9 \lambda / \beta \cos \theta$, where D is the average crystallite size, β is the full width half maxima, λ is the X-Ray wavelength and θ is the Bragg's angle. Lattice constant has been calculated from equation $a = d (h^2 + k^2 + l^2)^{1/2}$ where 'a' is lattice constant, d be the inter planar distance, hkl is miller indices. Lattice strain of $\text{Mn}_x\text{Ni}_{1-x}\text{Cr}_{0.5}\text{Fe}_{1.5}\text{O}_4$ were determined using the Williamson-Hall formula $\epsilon = \beta / 4 \tan \theta$, Where ϵ is the lattice strain of the structure [21, 22]. X-ray Density can be calculated by $\rho_x = ZM/\text{Na}^3$, Where Z is number of molecules per unit cell, here it is 8. M is Molecular weight of the sample; N is Avogadro's Number, 'a' lattice constant. Dislocation density has been found by using the relation $\delta = 15 \epsilon / a D$, here δ be the dislocation density. All these structural parameters are calculated and tabulated in TABLE 2.

The average crystallite size 'D' estimated for $\text{Mn}_x\text{Ni}_{1-x}\text{Cr}_{0.5}\text{Fe}_{1.5}\text{O}_4$ nanoferrites for different 'x' values lie in between 44 nm and 55 nm vary non-linearly. The samples having lattice constant between 8.4407 \AA and 8.6615 \AA and this increases in lattice constant in the samples is due to addition of higher ionic radius Mn^{2+} ion which replaces the smaller ionic radius Ni^{2+} ion ($r_{\text{Ni}} = 0.69 \text{ \AA}$) [23, 24]. Only $\text{Mn}_{0.6}\text{Ni}_{0.4}\text{Cr}_{0.5}\text{Fe}_{1.5}\text{O}_4$ violates Vegard's law, this behavior is due to point of inversion of mixed spinel, large dislocation (2.93×10^{15} lines/m), most strained lattices (3.65×10^{-3}) and low X-ray density value. Increase in Mn^{2+} concentration leads to increase in average crystallite size and lattice constant. Variation in the crystallite size is generally due to the influence of dopant, here crystallite size and lattice constant increase upto $x = 0.4$ concentration this due to Ni^{2+} and Mn^{2+} ions prefers octahedral sites whereas Fe^{3+} ions prefers both tetrahedral and octahedral sites. When the particle size reduced to nano dimension there is change in cation distribution Mn^{2+} occupies both tetrahedral and octahedral sites [25]. For concentration $x = 0.6$ crystallite size is maximum with value of 55.08 nm. These phenomena arise due to more strained and dislocated sublattice created by Manganese. Molecular weight of the $\text{Mn}_x\text{Ni}_{1-x}\text{Cr}_{0.5}\text{Fe}_{1.5}\text{O}_4$ composition increases with replacement of higher atomic mass (54.94 g) Mn^{2+} by lower atomic mass (58.69 g) Ni^{2+} in the composition and this matches with the X-Ray density values calculated from XRD profile.

B. Scanning Electron Microscope (SEM) and Energy Dispersive Spectroscopic (EDS) analysis

The morphological characteristics of the obtained $\text{Mn}_x\text{Ni}_{1-x}\text{Cr}_{0.5}\text{Fe}_{1.5}\text{O}_4$ nanoferrites sintered at 1173 K have been investigated with the help of VEGA 3 TESCAN for all concentration of the samples. Fig.2 shows morphology of $\text{Mn}_x\text{Ni}_{1-x}\text{Cr}_{0.5}\text{Fe}_{1.5}\text{O}_4$ nano ferrite samples for the increase in concentration of Manganese ($x = 0, 0.2, 0.4, 0.6, 0.8, 1.0$). The micrographs show the agglomerated grain structure with clusters of fine particle clinging together. The morphology is almost uniform and regular having spherical shaped particles for all the concentration except 0.4 and 0.6. Point of inversion Nickel and Manganese manipulated the morphology. Agglomeration is due to increase in magnetic interaction among the particles influenced by Mn^{2+} [26]. Thus results of SEM well in agreement with X-Ray diffraction pattern. Especially for $x = 0.4, 0.6, 1.0$ agglomeration is more, this matches with disappearance of minor reflection planes (111), (222) and (620) due to amorphization at the edges of the nanocrystal and it is obvious for higher temperature sintering. The surface of the ferrite samples has a number of fine pores or voids that are attributed to the large amount of Oxygen and chlorine gas liberated during the sintering process. Presence of vacancies results in contraction of Lattice even higher ionic radius dopant is added to the sample [27].

EDS spectrum for the $\text{Mn}_x\text{Ni}_{1-x}\text{Cr}_{0.5}\text{Fe}_{1.5}\text{O}_4$ ($x = 0, 0.2, 0.4, 0.6, 0.8, 1.0$) nanoferrites are recorded with BRUKER EDS and illustrated in Fig.3. The result shows each peak corresponds to the element added in the prepared nanoferrite which confirmed the presence of elements in respective concentration. Iron and oxygen are the major constituents in the composition, Manganese and Nickel is the next major constituent to the iron in the sample. It is interesting to note that the preparation condition completely favors the formation of mixed ferrite and allow us to study the effect of increasing the Mn content on the properties of the Ni-Cr

nano ferrite. The peak values variation is due to its stoichiometry, for all the concentration. The values of Nickel vary with the increase in Manganese concentration.

C. Fourier Transform Infrared Spectroscopy (FTIR) Analysis

Fourier transform infrared (FTIR) studies were carried out to ascertain the metal-oxygen bonding. FTIR spectrums of the investigated sample are shown in Fig.4 and corresponding peaks are tabulated in the Table 3. Infrared spectroscopy study supported the formation of Mn-Ni-Cr spinel nano ferrite with enlightening two strong absorption bands around 400 cm^{-1} and 600 cm^{-1} that are common features of all spinel ferrites [28]. The spinel structure is attributed to the stretching vibrations of the unit cell of the spinel in the tetrahedral (A) site and the metal-oxygen vibration in the octahedral (B) site. These absorption bands are highly sensitive to changes in interaction between oxygen and cations, as well as to the size of the obtained nano-particles [29]. The broadening of the spectral band depends on the statistical distribution of cations over A and B sites. The vibration frequency depends on the cation mass, cation-oxygen distance and bending force [30].

From Fig 4, Intrinsic stretching vibration frequency of metal-oxygen at tetrahedral site observed in a range 617 cm^{-1} - 601 cm^{-1} and its value shifting linearly towards lower frequency with increase in Mn^{2+} concentration in the samples. And replacement of Ni^{2+} ions by bigger Mn^{2+} in octahedral sites in Manganese doped Nickel-Chromium ferrite results in a slight increase in metal oxygen bond length and consequently decrease the wave number of octahedral and tetrahedral sites by increasing substitution content [31, 32]. No octahedral peak observed in the range of 443 cm^{-1} in concentration values of $x = 0.6$. Intensity of the peaks corresponds to octahedral and tetrahedral bonds increases for $x \leq 0.6$ and decreases for 0.8 and 1.0 concentration with the addition of Mn^{2+} content. It is well known that the intensity ratio is function of change of dipole moment with the internuclear distance. This value represents the contribution of ionic bond Fe-O in the lattice. So the observed increase and decrease in the absorption band intensity with increase in Manganese content, is due to perturbation occurring in Fe-O bonds. The electronic distribution of Fe-O bonds greatly affected by the dopant Mn^{2+} which is having comparatively bigger radius and high atomic weight (Mn-55.94 a.m.u, Ni 58.69 a.m.u)[33].

D. Vibrational Sample Magnetometer (VSM) analysis

MH-loops reveals the magnetic properties of $\text{Mn}_x\text{Ni}_{1-x}\text{Cr}_{0.5}\text{Fe}_{1.5}\text{O}_4$ nanoferrites ($x = 0, 0.2, 0.4, 0.6, 0.8, 1.0$). Hysteresis loops for the samples are recorded with LAKESHORE Vibrational sample magnetometer at 300 K with applied field as 20 KOe are shown in Fig.5. The value of anisotropy constant was calculated from Stoner-Wohlfarth relation as follows $H_c = K/M_s$ [34], Where H_c is the coercivity, M_s saturation magnetization and K magnetic anisotropy constant. Calculation of magnetic moment in Bohr magneton was carried out using the following relation, $n_B = (\text{Molecular Weight} \times M_s) / 5585$ [35].

Magnetic parameters saturation magnetization (M_s), Remanence Magnetization (M_r), Coercivity (H_c), Squareness ratio, Magnetic anisotropy constant (K) and magneton number are calculated from Hysteresis loop and tabulated in Table 6. Generally magnetic properties in the prepared sample arise from coupling between spin and orbital angular momentum (L-S coupling) and electron spin (S-S coupling) [36]. In the case of spinel nano magnetic ferrite material magnetic parameters are influenced by cation distribution, collinearity and non-collinearity (canting) of spins on their surface, crystallite size and dopant. In present study all the concentration of Mn^{2+} in Nickel-Chromium nano ferrite the hysteresis loops show similar behaviour where the magnetization first increases abruptly with increase in the field up to 1000 Oe and then increase slowly and saturates at nearly 2500 Oe of the applied magnetic field.

From the M-H loop and Table.4, Saturation magnetization M_s value increases upto 0.4 Mn concentration in the sample due to addition of Higher Bohr magneton Manganese ions in the sample. For higher concentration 0.6, 0.8 and 1.0 of Mn, saturation magnetization value decrease this is due to lowering of Fe ions in the composition and it disturbs total magnetic moment of the sample by cancelling each other. Coercivity decreases due to the influence of Mn^{2+} ion in the sample and variation in crystallite size. But Remanence value changes non linearly with respect to Mn^{2+} ion in the sample. This is due to more number of incorporation of Mn^{2+} ion on the sublattices. Bohr magneton value also increase with increase in Mn ion upto 0.4 concentration, for more than 0.4 concentration of Manganese in Nickel-Chromium nano ferrite, Fe^{2+} ion with magnetic moment ($4.90\mu_B$) in octahedral site reduced into Fe^{3+} ion with magnetic moment ($5.92\mu_B$) this is due to migration of these ions and also decrease in Nickel at octahedral site. All the sample shows super-paramagnetic behavior. The appearance of super-paramagnetism indicates that the magneto crystalline anisotropy, which is important to hold magnetic ions in certain direction, has been overcome by thermal energy [37]. The magnetic anisotropy constant is maximum for the concentration 0.6 and 0.4 and high crystallinity is possible in disordered spinel structure. Ordered spinel structure has low value of magnetic anisotropy constant.

IV. CONCLUSION

Manganese doped Nickel-Chromium nano ferrite at various concentrations has been successfully synthesized by uncomplicated and cheap co-precipitation method. Average crystallite size lies between 44nm and 55nm. All physical properties are studied for samples sintered at 1173K. Addition of Mn^{2+} ion influenced the structural properties such as Average crystallite size, lattice constant, lattice strain, dislocation density and X-Ray density of the synthesized samples. Absence of super structure reflection peaks from XRD analysis suggests that nano crystal lattice having disordered spinel structure in the higher concentration of the dopant. SEM shows morphology manipulated by Mn^{2+} ion in the sample and FTIR observation have fine match with results of XRD and SEM. From VSM analysis and Low concentration of Mn^{2+} induced magnetic ordering and crystal disordering. Higher concentration of Manganese induces most disordered magnetic structure which is found from its magnetic anisotropy constant value. Important finding in this work is 0.6 and 0.4 concentration of Manganese in Ni-Cr in nano ferrite has its maximum magnetic anisotropy constant value, which will release more thermal energy in alternating magnetic field, and should be act as best candidate for magnetic fluid hyperthermia and in targeted drug delivery system.

REFERENCES

- [1] Carta.D, Marras.C, Loche.D, Mountjoy.G, Ahmed.S.I, Corrias.A, The journal of chemical physics 138 (2013) 054702.
- [2] Manikandan.A, Vijaya.J.J, Sundararajan.M, Meganathan.C, John Kennedy.L, Bououdina.M, Superlattices and Microstructures 64 (2013) 118-131
- [3] Ichiyanagi.Y, Kubota.M, Moritake.S, Kanazawa.Y, Yamada.T, Uehashi.T, Journal of magnetism and magnetic materials 310 (2007) 2378-2380.
- [4] Koseoglu.Y, Alan.F, Tan.M, Yilgin.R, Ceramic Inter. 38 (2012) 3625-3634
- [5] Camley.R.E, Celinski.Z, Fal.T, Glushchenko.A.V, J. Magn. Magn. Mate. 321 (2009) 2048-2054
- [6] Lee.J.H, Jang.J, Choi.J, Moon.S.H, Noh.S, Kim.J, Kim.I, Park.K.I and Cheon.J.Nat.Nanotechnol 6 (2011) 418-422
- [7] B.D.Culity, Elements of X-ray diffraction Chapter 14 (London, Addison-Wesley publishing company.Inc.,1976) (Chapter 14).
- [8] C.Kittel, Introduction to Solid State Physics 7thed (USA, John Willey publishing company, 1956).
- [9] A.Goldman, Modern Ferrite technology, 2nd ed., (New York , Springer Science Business Media Inc., 2006).
- [10] Zhao.L, Yang.H, Yu.L, Cui.Y.E, J.Mater. Sci., 42 (2007) 686 – 691.
- [11] Ranjithkumar.E, Aleksandr.S.Kamzin, Prakash.T, J.Magn. Magn. Mater. 378 (2015) 389-396
- [12] Misra.R.D.K, Gubbala.S, Kale.A, Mater.Sci.Eng.B 111 (2004) 164-174
- [13] Hassan.H.E, Sharshar.T, Hessien.M.M, Hemeda.O.M, Nuclear instruments and Methods in Physics Research B 304 (2013) 72-79
- [14] T.F.Marinca, I.Chicinas, O.Isnard, V.Pop, F.Pop, J.Alloy., and compounds, 509 (2011) 7931-7936.
- [15] Uthayakumar.B, Sukandhiya.S, Suryakumary.J, Periandy.S, IOSR Journal of Applied Physics, 9 ver III (2017) 5-12.
- [16] C.G.Ammankutty., S.Sugunna, J.App.Catal.A Gen 218 (2001) 39
- [17] S.R.Dhage ,Y.Khollam, S.B.Deshpande, V.Ravi., Mater. Res.Bull.38 (2003) 1601-1605.
- [18] B.P.Ladgaonkar, A.S.Vaigainkar, Materials chemistry and physics 56 (1998) 280-283.
- [19] C.S.Narasimhan and C.S. Swamy, Physica status solidi 59 (1980) 817
- [20] G.Sathishkumar.,C.Venkataraju., K.Sivakumar, Material Sciences and Applications 1 (2010) 19-24
- [21] E.Wolska, P.Piszora, W.Nowicki, J.Darul, Int.J.Inorganic Mater., 3 (2001), 503-507.
- [22] G.K.Williamson, W.H.Hall ,Acta Metall.1(1953) 22-31.
- [23] A.Kohrsand Zak, W.H.Abd.Majid, M.E. Abrishami, RaminYousefi, Solid State Sci.13 (2011) 251-256.
- [24] Tan.X., Li, G., Zhao, Y., Hu, C. Mater. Res. Bull.44, (2009) 2160.
- [25] Singhal.J, Singh.S, Barthwal.K, Chandra.K, Journal of solid state chemistry 178 (2005) 3183-3189.
- [26] S.Rahman, K.Nadeem, M.A.Rehman, M.Mumtaz, S.Naeem, I.L.Ipst,Ceram.Int. 39 (2013) 5235-5239
- [27] S.Prabakar, and M.Dhanam, J.Cryst.Growth, 41 285 (2005) 1-2
- [28] Hashim.M, Alimuddin, Shirsath.S.E, Kumar.S, Kumar.R, Roy.A.S, Shah.J, and Kotnala.R.K, Journal of alloys and compounds, 549 (2012) 348-357.
- [29] Farid.M, Ahmad.I, Aman.S, Kanwal.M, Murtaza.G, Alia.I, Ishfaq.M, Journal of Ovonic research 11 (2015) 1
- [30] Wahba.A.M, Mohammad.M.B, Ceramic International, 40 (2014) 6127-6135
- [31] Boshale.A.G, Chougule.B.K, Material chemistry and physics 97 (2006) 273
- [32] Smit.J, And H.P.J ijn.Ferrite(1959)
- [33] Shirsath.S.E, Toksha.B.G, Kadam.R.H, Patange.S.M, Mane.D.R, Jangam.G.S, Ghasemi.A, J.Physics chemistry of solids 71 (2010) 1669
- [34] Singh.N, Agrawal.A, Sanghi.S, Singh.P, Physica B, 406 (2011) 687
- [35] Singhal.S, Chandra.K, J.Solid state Chem. 180 (2007) 296
- [36] Gabbal.M.A, Angari.Y.M.A, Material chem. Physics 118 (2009) 153
- [37] Verma.A, Goel.T.C, Meadiratta.R.G, Kishan.P, Journal of Magnetism and magnetic material 208 (2000) 13-19.

TABLE 1: Comparison of X-Ray Intensity

Mn content 'x'	Composition	I ₂₂₀	I ₄₄₀
0.0	Ni _{1.0} Cr _{0.5} Fe _{1.5} O ₄	34.10	32.58
0.2	Mn _{0.2} Ni _{0.8} Cr _{0.5} Fe _{1.5} O ₄	32.27	46.87
0.4	Mn _{0.4} Ni _{0.6} Cr _{0.5} Fe _{1.5} O ₄	35.28	42.88
0.6	Mn _{0.6} Ni _{0.4} Cr _{0.5} Fe _{1.5} O ₄	33.85	45.61
0.8	Mn _{0.8} Ni _{0.2} Cr _{0.5} Fe _{1.5} O ₄	35.06	41.02
1.0	Mn _{1.0} Cr _{0.5} Fe _{1.5} O ₄	39.72	53.23

TABLE 2: Structural parameters of Mn_xNi_{1-x}Cr_{0.5}Fe_{1.5}O₄ for various concentrations sintered at 1173K

Mn content 'x'	Composition	Crystallite Size D (nm)	Lattice Constant a (Å)	Molecular Weight g/mole	X-ray density g/cm ³	Lattice strain 10 ⁻³	Dislocation Density 10 ¹⁵
0.0	Ni _{1.0} Cr _{0.5} Fe _{1.5} O ₄	44.74	8.4407	232.405	5.1340	2.48	1.68
0.2	Mn _{0.2} Ni _{0.8} Cr _{0.5} Fe _{1.5} O ₄	54.13	8.4942	231.653	5.0213	2.21	0.778
0.4	Mn _{0.4} Ni _{0.6} Cr _{0.5} Fe _{1.5} O ₄	52.41	8.5156	230.901	4.9674	2.17	0.836
0.6	Mn _{0.6} Ni _{0.4} Cr _{0.5} Fe _{1.5} O ₄	55.08	8.6263	230.149	4.7631	3.65	2.93
0.8	Mn _{0.8} Ni _{0.2} Cr _{0.5} Fe _{1.5} O ₄	47.97	8.6110	229.397	4.7728	2.64	1.20
1.0	Mn _{1.0} Cr _{0.5} Fe _{1.5} O ₄	46.42	8.6615	228.645	4.6745	2.50	0.999

TABLE 3: Vibrational frequency of octahedral and tetrahedral sites

Mn content 'x'	Composition	v ₁ tetra	v' ₁ tetra	v ₂ octa	v' ₂ octa
0.0	Ni _{1.0} Cr _{0.5} Fe _{1.5} O ₄	614.01	495.76	443.25	-
0.2	Mn _{0.2} Ni _{0.8} Cr _{0.5} Fe _{1.5} O ₄	609.22	491.00	427.48	415.03
0.4	Mn _{0.4} Ni _{0.6} Cr _{0.5} Fe _{1.5} O ₄	605.66	-	420.80	-
0.6	Mn _{0.6} Ni _{0.4} Cr _{0.5} Fe _{1.5} O ₄	595.71	-	-	-
0.8	Mn _{0.8} Ni _{0.2} Cr _{0.5} Fe _{1.5} O ₄	587.75	471.54	-	-
1.0	Mn _{1.0} Cr _{0.5} Fe _{1.5} O ₄	582.32	470.25	-	-

TABLE 4: Magnetic parameters of $Mn_xNi_{1-x}Cr_{0.5}Fe_{1.5}O_4$ for various concentrations sintered at 1173K

Mn content 'x'	Composition	M_s (emu/g)	M_r (emu/g)	H_c (Oe)	M_r/M_s	K (erg/cm ³)	n_B
0.0	$Ni_{1.0}Cr_{0.5}Fe_{1.5}O_4$	29.21	13.21	316.5	0.452	9244.97	1.215497
0.2	$Mn_{0.2}Ni_{0.8}Cr_{0.5}Fe_{1.5}O_4$	50.82	31.52	122.2	0.620	6210.20	2.107897
0.4	$Mn_{0.4}Ni_{0.6}Cr_{0.5}Fe_{1.5}O_4$	73.72	43.77	144.4	0.594	10645.17	3.03605
0.6	$Mn_{0.6}Ni_{0.4}Cr_{0.5}Fe_{1.5}O_4$	60.85	38.21	188.8	0.628	11488.48	2.50753
0.8	$Mn_{0.8}Ni_{0.2}Cr_{0.5}Fe_{1.5}O_4$	41.60	21.69	55.5	0.521	2308.8	1.70867
1.0	$Mn_{1.0}Cr_{0.5}Fe_{1.5}O_4$	43.75	31.41	55.5	0.718	2428.13	1.79109

M_s - Saturation magnetization; M_r - Remanent Magnetization; H_c - Coercivity; K - Magneto Crystalline Anisotropy; n_B -Magneton Number

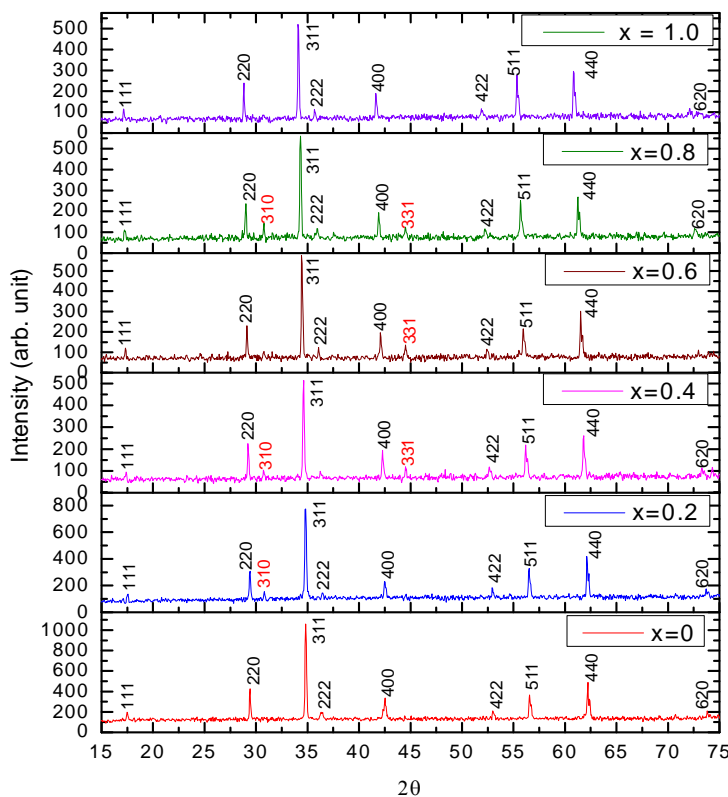


Figure 1: X-Ray Diffraction pattern of Mn Doped Ni-Cr nano ferrite samples

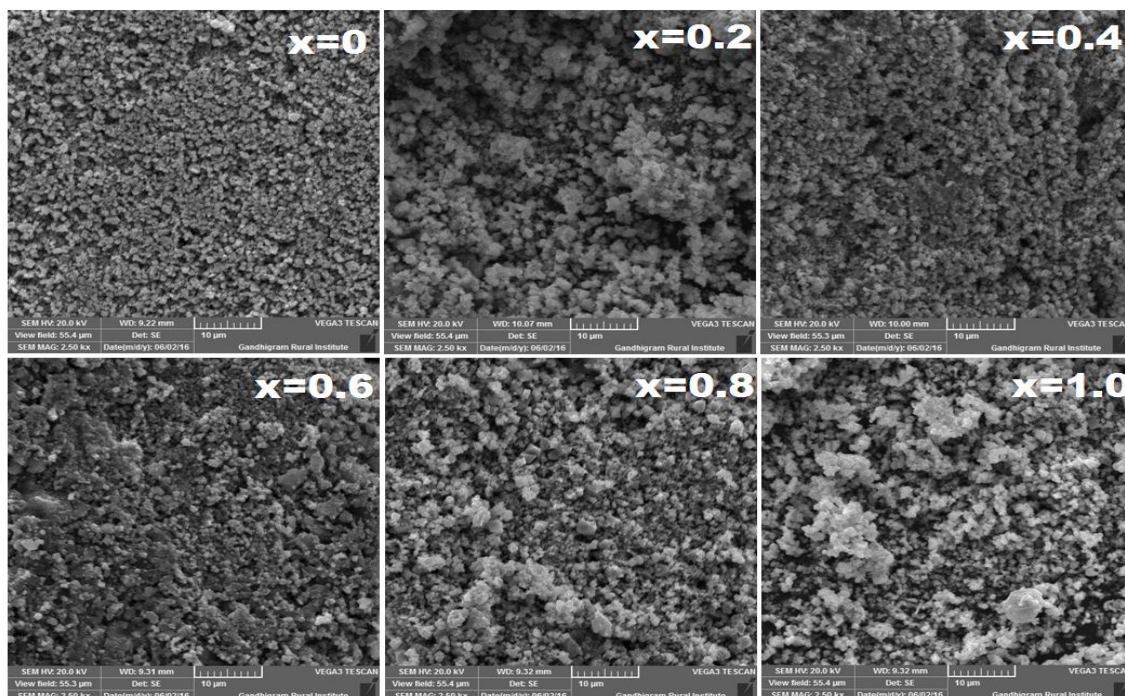


Figure2. SEM micrograph of $Mn_xNi_{1-x}Cr_{0.5}Fe_{1.5}O_4$ ($x = 0(a), 0.2(b), 0.4(c), 0.6(d), 0.8(e), 1.0(f)$) nanoferrite sintered at 1173K

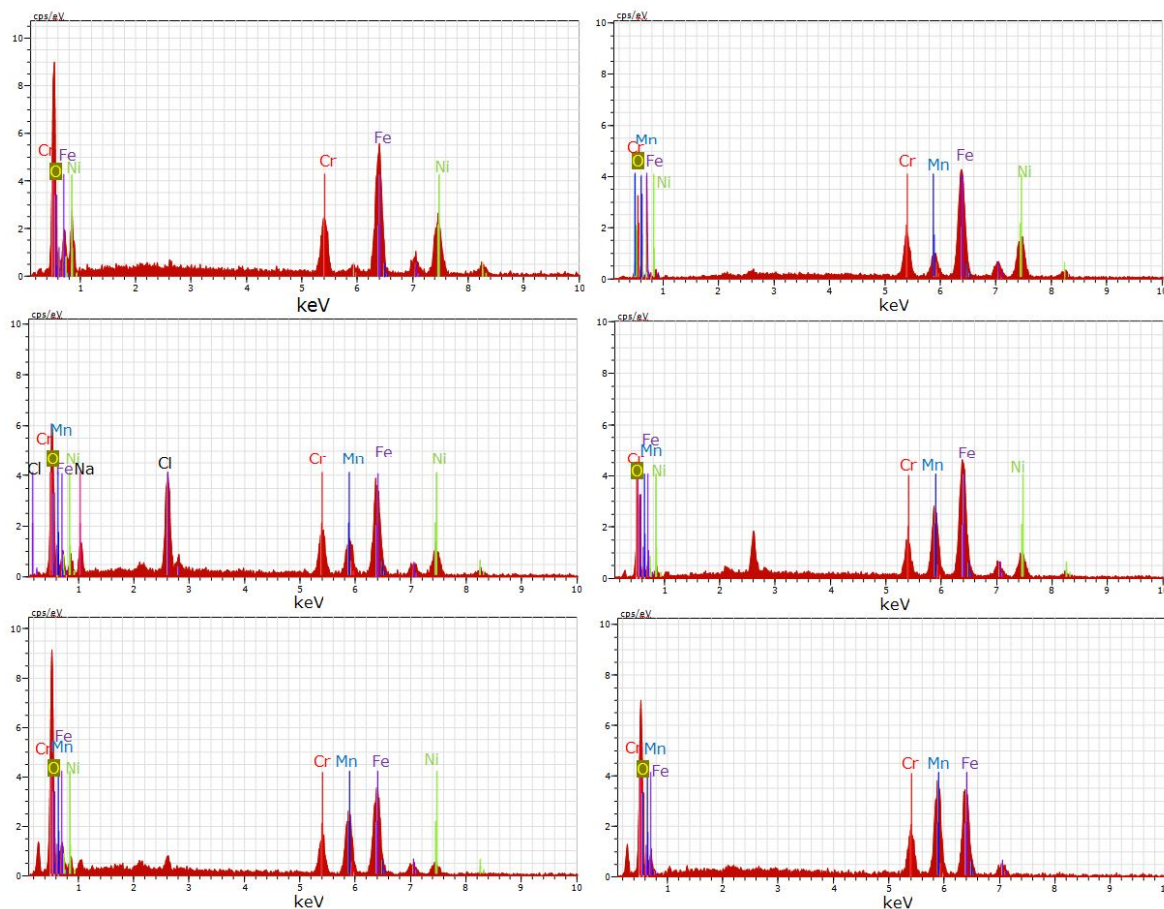


Figure 3. EDS of $Mn_xNi_{1-x}Cr_{0.5}Fe_{1.5}O_4$ ($x = 0, 0.2, 0.4, 0.6, 0.8, 1.0$) nanoferrite sintered at 1173K

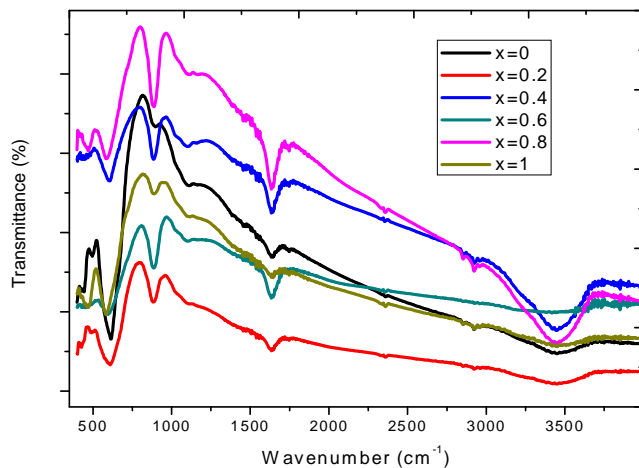


Figure 4. FTIR spectra of $Mn_xNi_{1-x}Cr_{0.5}Fe_{1.5}O_4$ ($x = 0, 0.2, 0.4, 0.6, 0.8, 1.0$) nanoferrite sintered at 1173K

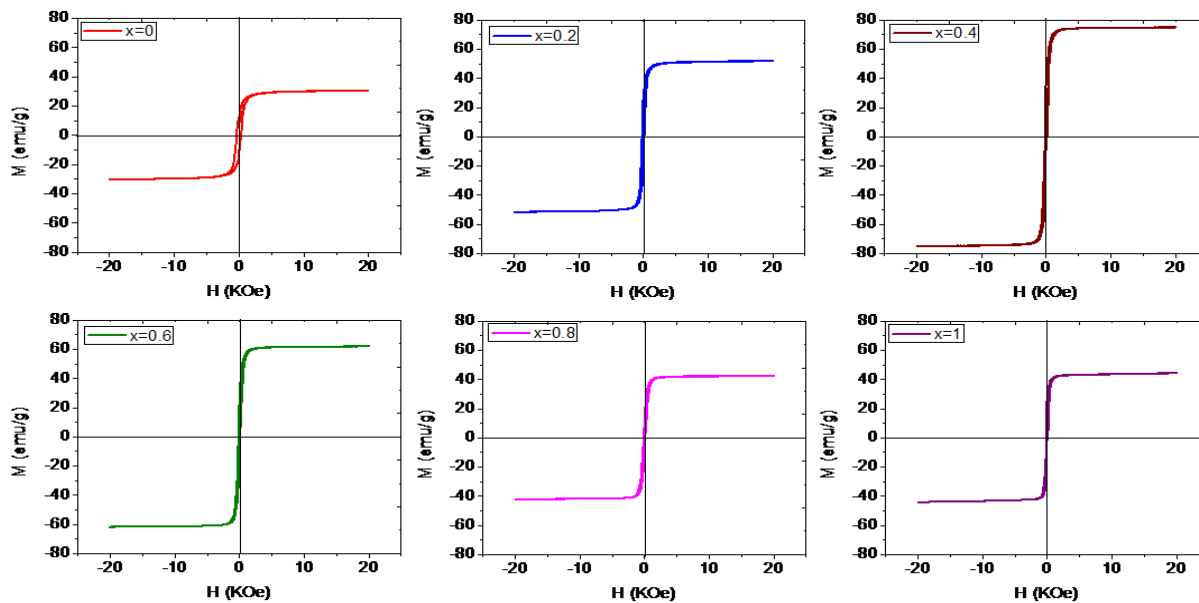
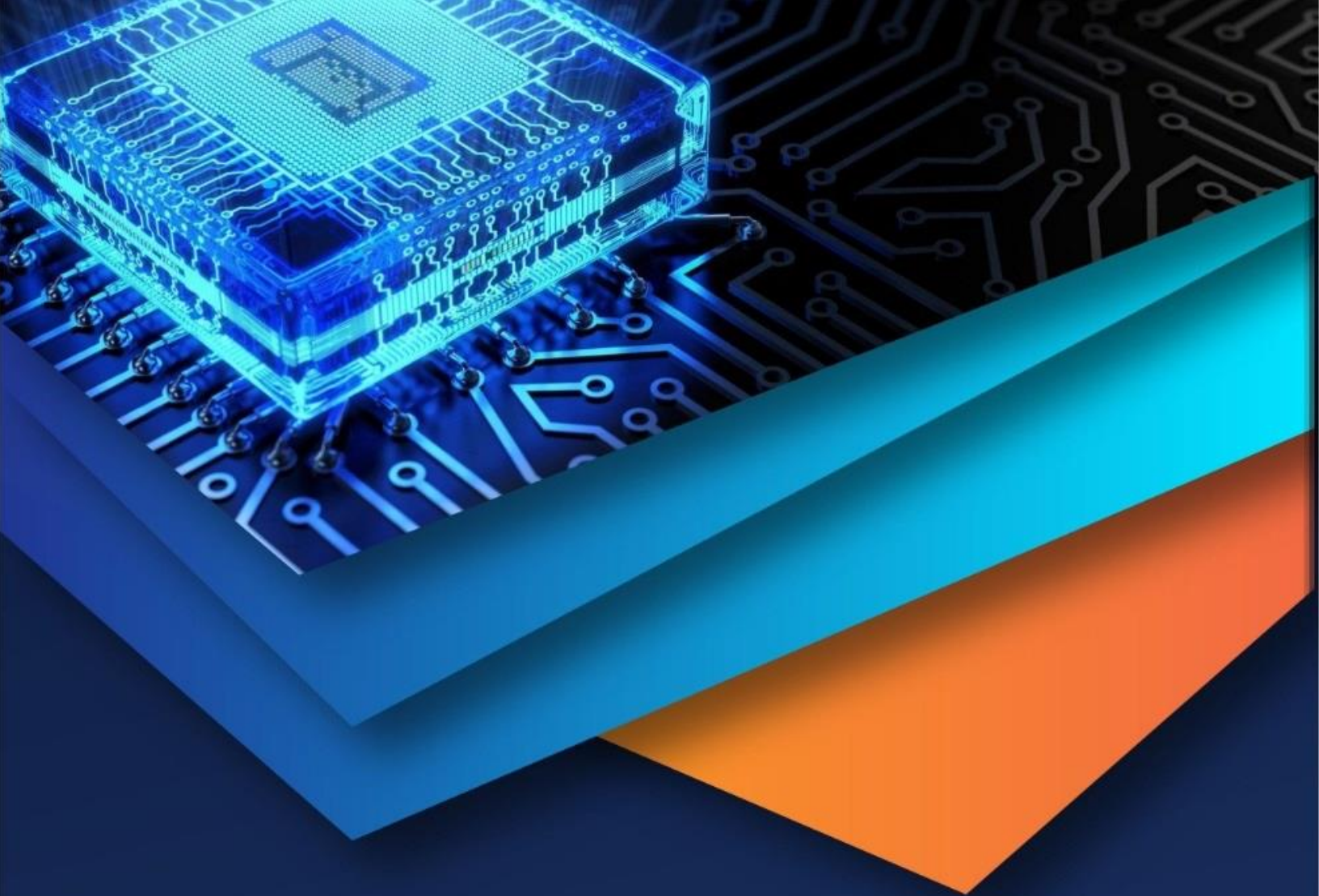


Figure 5. Magnetic hysteresis curves of $Mn_xNi_{1-x}Cr_{0.5}Fe_{1.5}O_4$ ($x = 0, 0.2, 0.4, 0.6, 0.8, 1.0$) sintered at 1173K



10.22214/IJRASET



45.98



IMPACT FACTOR:
7.129



IMPACT FACTOR:
7.429



INTERNATIONAL JOURNAL FOR RESEARCH

IN APPLIED SCIENCE & ENGINEERING TECHNOLOGY

Call : 08813907089  (24*7 Support on Whatsapp)